departure from two-dimensionality. Another factor which can significantly affect the value of Π that will be obtained from a given profile is the length scale δ_c used to nondimensionalize the y coordinate when plotting the velocity defect profile.

Figure 1 shows a typical generalized velocity distribution in law of the wall coordinates reduced from the tabulated data of Ref. 11. The constants in Eq. (2) ($k=0.43$, $C=5.5$) have been found to be representative of hypersonic turbulent profiles in helium. They are consistent with values to be found in the literature, e.g., $k=0.41$, $C=4.9$ from Ref. 5, and $k=0.43$, $C=6$ from Ref. 8. Noted in the figure are δ, δ_c, u_e^*, and u_c^*. Unlike incompressible and most supersonic turbulent boundary layers, δ/δ_c is 1.5 for the profile shown.

Twelve boundary-layer profiles from Ref. 11 were reduced to generalized velocity defect form using measured skin friction values for calculating u_τ. Values of δ_c for each profile were obtained from plots similar to Fig. 1. The velocity defect region of the boundary layer of Fig. 1 is compared with Eqs. (3) and (4) in Fig. 2 for several values of the wake constant Π. The value of Π for this profile was 0.43, as found by trial-and-error variation of Π until Eq. (3) fits the data. This value is significantly smaller than the high Reynolds number limit of 0.55; however, $\delta u_\tau/\nu_w$ was only 290, indicating the boundary layer to be in the region of low Reynolds number effects. This is evident in Fig. 3 where the variation of Π with $\delta u_\tau/\nu_w$ taken from the tabulation of Ref. 1 for incompressible turbulent boundary layers is shown along with the present Mach 11 data.

Although the present values of Π are greater than Coles' incompressible values, they are lower than the mean value of 0.81 from Ref. 8, and, in addition, exhibit the same trend as incompressible data, a decrease with decreasing $\delta u_\tau/\nu_w$. At $T_w/T_t=0.34$-0.4, Π is closer to the incompressible relation than for the hotter wall data. If inferred instead of measured values of c_f had been used to obtain u_τ, the derived values of Π at cold wall conditions would have been more in agreement with the hot wall data.

All data were originally reduced using δ as the length scale for nondimensionalizing y when plotting the velocity defect. Values of Π obtained by this method were found to be lower than corresponding incompressible values at the same Reynolds number. Since δ_c is the correct length scale to use, only data reduced using δ_c are presented here. The difference in the present data at Mach 11.4 (equivalent to an air boundary layer at Mach 14.7 in terms of density ratio) and the the incompressible is not large when compared with the wide variation in incompressible values of Π found in Ref. 1.

References

[1] Coles, D.C., "The Turbulent Boundary Layer in a Compressible Fluid," R-403-PR, The Rand Corporation, Santa Monica, Calif., 1962.

[2] Van Driest, E.R., "Turbulent Boundary Layer in Compressible Fluids," *Journal of the Aeronautical Sciences*, Vol. 18, 1951, pp. 145-160, p. 216.

[3] Bushnell, D.M., Cary, Jr., A.M., and Harris, J.E., "Calculation Methods for Compressible Turbulent Boundary Layers-1976," NASA SP-422, 1977.

[4] Coles, D.E., "The Law of the Wake in the Turbulent Boundary Layer," *Journal of Fluid Mechanics*, Vol. 1, 1956, pp. 191-226.

[5] Baronti, P.O. and Libby, P.A., "Velocity Profiles in Turbulent Compressible Boundary Layers," *AIAA Journal*, Vol. 4, Feb. 1966, pp. 193-202.

[6] Watson, Ralph D., "Wall Cooling Effects on Hypersonic sitional/Turbulent Boundary Layers at High Reynolds Numbers," *AIAA Journal*, Vol. 15, Oct. 1977, pp. 1455-1461.

[7] Hopkins, E.J., Keener, E.R., Polek, T.E., and Dwyer, H.A., "Hypersonic Turbulent Skin-Friction and Boundary-Layer Profiles on Nonadiabatic Flat Plates," *AIAA Journal*, Vol. 10, Jan. 1972, pp. 40-48.

[8] Danberg, J.E., "A Re-evaluation of Zero Pressure Gradient Compressible Turbulent Boundary Layer Measurements," BRL Rept. No. 1642, U.S. Army Ballistic Research Laboratories, Aberdeen Proving Ground, Md., April 1973, AD-762152.

[9] Maise, G. and McDonald, H., "Mixing Length and Kinematic Eddy Viscosity in a Compressible Boundary Layer," *AIAA Journal*, Vol. 6, Jan. 1968, pp. 73-80.

[10] Bull, M.K., "Velocity Profiles of Turbulent Boundary Layers," *The Aeronautical Journal of the Royal Aeronautical Society*, Vol. 73, Feb. 1969, pp. 143-147.

[11] Watson, R.D., "Characteristics of Mach 10 Transitional and Turbulent Boundary Layers," NASA TP-1243, 1978.

Optimization of Triangular Laced Truss Columns with Tubular Compression Members for Space Application

Chai Hong Yoo*
Marquette University, Milwaukee, Wisc.

Introduction

LARGE space structures built up from a series of long columns to form a stiff skeletal framework are being considered for a number of NASA's future missions[1] such as solar cell platforms or antenna farms. The structural elements of such large space structures are characterized by low loading and minimum gage construction. Euler buckling load is a prominent design consideration. However, minimum gage for production and fabrication frequently is the limiting factor. Due to the obvious reason for minimizing the weight of the structures, optimization is usually considered in terms of minimum weight. As one of the most weight-efficient compression components of large space structures,[2] a tubular laced column is investigated in this study.

The optimization procedures are based on designing for a column with initial imperfections. Initial imperfections associated with columns conceived for space application yield significant implication, since the column behavior is very sensitively affected by these imperfections. These imperfections can result from a number of different causes such as manufacturing in the orbit, thermal gradients, lateral accelerations, and impact during docking. Mikulas[2] made a similar study based on four different column configurations. A comparison of the results of these studies will be shown and the design of diagonals and battens will be discussed.

Truss Geometry

The triangular laced truss column is fabricated with three thin-walled tubular longitudinals placed at each vertex of an isotriangle, which are braced with tubular battens and laced double diagonals in each side of the bay as shown in Fig. 1.

The side length of the isotriangle is readily obtained from the geometry as

$$S=L/N\tan\theta \quad (1)$$

where L is the column length through which the load must be transmitted, N is the number of bays, and θ is the angle between the batten and the diagonal as defined in Fig. 1. The moment of inertia for the truss cross section is:

$$I=A_L S^2/2=A_L L^2/2N^2\tan^2\theta \quad (2)$$

Received Sept. 19, 1978; revision received Feb. 27, 1979.

Index categories: Structural Design; Computational Methods.

*Asst. Professor, Dept. of Civil Engineering.

where $A_L = \Pi D_L t_L$ is the cross-sectional area and D_L and t_L are the diameter and thickness (minimum) of the longitudinal, respectively.

Truss Design

Design of Longitudinal

The initial moment (M_{init}) in a beam column is magnified by[3]

$$M_{\max} = \frac{M_{\text{init}}}{1-P/P_E} = \frac{Pa}{1-P/P_E} \tag{3}$$

where a is the maximum amplitude of the initial imperfection at the midheight of the column, P is the design load, and P_E is the Euler buckling load.

The maximum load on the highly loaded longitudinal is then

$$P_L = \frac{P}{3} + \frac{M_{\max} c A_L}{I} \tag{4}$$

where c is the extreme fiber distance and is obtained by:

$$c = \sqrt{3}L/3N\tan\theta \tag{5}$$

Since P_L must not exceed the Euler load within each bay, it may be written as

$$P_L = \frac{\Pi^2 E(\Pi D_L^3 t/8)C_L}{\text{FS}(L/N)^2} \tag{6}$$

wheere FS stands for a factor of safety, E is Young's modulus, and C_L is a fixity coefficient ($1 \le C_L \le 4$) normally specified equal to one to simulate the pin-ended boundary conditions. Substituting these relationships into Eq. (4) yields

$$\frac{\Pi^3 E D_L^3 t N^2 C_L}{8L^2 \text{FS}} = \frac{P}{3} + \frac{2PaN\tan\theta}{(\sqrt{3}L)\left(1 - \dfrac{2PN^2\tan^2\theta}{\Pi^3 E D_L t}\right)} \tag{7}$$

Equation (7) is then solved for the diameter of the longitudinal D_L under a given imperfection a and a proper factor of safety. The number of bays N and the angle θ are determined by iterations which result in minimizing the total column mass.

It has been observed that the overall column mass decreases somewhat proportional to the minimum thickness specified. However, minimum thickness is limited, not simply because of the production capability of current technology, but also because of the local crippling criterion. The limiting stress of an isotropic cylinder is given by Ref. 4 as a function of D_L/t:

$$f_{cr} = \frac{2\beta E}{\sqrt{3(1-\mu^2)}D_L/t} \tag{8}$$

where $\beta = 1\text{-}0.901(1-e^{-\phi})$ and $\phi = (1/16)(\sqrt{D_L/2t})$.

In general, this crippling check may not be necessary except for longitudinals consisting of extremely thin (10 mil or lower) tubes subjected to fairly high loads. It is likely that a graphite/epoxy column of this type will have primary ply layup in the axial direction, thus resulting in highly orthotropic construction, for which Eq. (8) may not be exactly valid. However, for these limiting cases, Eq. (8) seems appropriate to use as an approximate check rather than utilizing a lengthy expression for crippling stress in an orthotropic material.

Design of Diagonal

The diagonal consists of two wire-rope-type tension members to carry the maximum shearing force at the ends of the column. The maximum shearing force is given by Ref. 3 as:

$$Q_{\max} = \frac{Pa\Pi/L}{1-P/P_E} \tag{9}$$

From equilibrium considerations the maximum load in a diagonal is:

$$P_D = \frac{Pa\Pi/L}{\sqrt{3}\cos\theta(1-P/P_E)} \tag{10}$$

This load may be used for sizing the diagonals for strength requirement.

Following the long procedure outlined in Ref. 5 and considering the shear deformation, the load-carrying capacity of the laced column under this study can be expressed as:

$$P_{cr} = \frac{\Pi^2 E_L I}{L^2} 1 \Big/ \left\{ 1 + \frac{2}{3}\left[\frac{\Pi^2 E_L INS}{L^3}\right]\left[\frac{1}{E_D A_D \tan^3\theta} + \frac{1}{E_B A_B}\right]\right\} \tag{11a}$$

or

$$P_{cr} = \Pi^2 E_L I/(kL)^2 \tag{11b}$$

where subscripts L, D, and B stand for longitudinals, diagonals, and battens, respectively. Assuming one material is used for all members, k may be written as:

$$k = \left[1 + \frac{2}{3}\frac{\Pi^2 INS}{L^3}\left(\frac{1}{A_D\tan^3\theta} + \frac{1}{A_B}\right)\right]^{1/2} \tag{12}$$

It has been observed that the load-carrying capacity of the column decreases markedly (some 10-25%) due to shear deformation effect when the slenderness ratio is in the vicinity of the lower limiting value of the Euler formula. After a series of trial evaluations, the following formulas seem appropriate to use for sizing the diagonal for stiffness:

$$A_D = -\frac{A_L}{30\text{LSR}}(L/r) + \frac{2}{15}A_L \quad (\text{for } L/r \le 3\text{LSR}) \tag{13a}$$

$$A_D = \frac{A_L}{30} \quad (\text{for } L/r > 3\text{LSR}) \tag{13b}$$

where r is the radius of gyration and LSR is the lower limit of slenderness ratio below which the Euler formula is invalid. The area of the diagonal is determined either by Eq. (10) or Eq. (13), whichever gives the higher value.

Design of Battens

The ideal batten stiffness is given by Ref. 6 as:

$$K_{id} = \alpha P_L N\sqrt{C_B}/L \tag{14}$$

where α is a function of the number of bays. α approaches asymptotically to four for columns with more than five bays. C_B is the fixity coefficient of the batten. The strength requirement of a batten as a bracing is[6]

$$P_{br} = a\frac{K_{id}}{1-K_{id}/K_{act}} \tag{15}$$

where K_{act} is the stiffness actually provided. Usually K_{act} is taken equal to twice of K_{id} and a is estimated somewhere between $L_B/250$ and $L_B/500$ (Ref. 6). Assuming $a = L_B/400$, $L_B = L/N$ and using Eqs. (14) and (15) yields

$$P_{br} = 8\sqrt{C_B}P_L/400 \tag{16}$$

Using $C_B = 1$ to simulate the pin-ended condition, Eq. (16) gives

$$P_{br} = 0.02P_L \tag{17}$$

The compressive force that develops in the batten is:

$$P_B = P_D \cos\theta \tag{18}$$

Hence, the design load for the batten is given by either Eq. (17) or Eq. (18), whichever results in a larger value.

According to Shanley,[7] the optimal stress level in cylindrical tubes is given by:

$$f = \left[\frac{P_B \Pi k_2 E^2 C_B}{8S^2}\right]^{1/3} \tag{19}$$

Hence, $A_B = P_B / f$ and the diameter of the batten may be expressed as:

$$D_B = \left[\frac{A_B^2 (k_2^2 ES^2 / \Pi P_B C_B)^{1/3}}{\Pi}\right]^{1/2} \tag{20}$$

where the coefficient k_2 is a function of Poisson's ratio. The optimum thickness of the batten is then

$$t_B = A_B / (\Pi D_B) \tag{21}$$

More often than not the t_B given by Eq. (21) is thinner than the minimum gage specified. If such is the case, the diameter of a batten is obtained by the Euler equation.

Truss Mass

Assuming one material is used for longitudinals, diagonals, and battens, the total column mass is:

$$M = 3\rho_m [\Pi D_L t_{\min} L + (N+1) \Pi D_B t_{\min} S + 2NA_D (S/\cos\theta)] \tag{22}$$

where ρ_m is mass density. The procedure for obtaining minimum mass column is as follows:

1) Input all constants such as L, E, $t_{\min}$, C_L, C_B, etc.

2) Assume values for N and θ in reasonably wide ranges and solve for D_L using Eq. (7).

3) Check D_L against all constraints. If it is satisfactory, proceed to step 4; otherwise, discard this set of N and θ and go back to step 2.

4) Compute all necessary values for Eq. (22) and store.

5) Repeat steps 2-4.

6) Sort out the minimum column mass. The computer time (CPU) required for this iteration is manageable. By using wide ranges of double DO-LOOP indexes (for example, $N = 1$-10,000, $\theta = 1$-89 deg), the possibility of overlooking the optimal solution can be effectively eliminated.

Results and Discussion

The optimum design procedures developed herein were carried out on a graphite/epoxy column 10-500 m long and subjected to loading from 1000 N to 25,000 N with initial imperfection ratios ranging from 0-0.004. The material properties were taken from Ref. 8 as $E = 143$ GN/m^2, $f_y = 323$ MN/m^2, $G = 6$ GN/m^2, $\rho_m = 1744$ kg/m^3. The minimum material thicknesses were 2.54×10^{-4} m (10 mil), 3.81×10^{-4} m (15 mil), and 5.08×10^{-4} m (20 mil). Specific findings are:

1) Imperfections reduce column load-carrying capacity up to 50% of Euler load where the imperfection is only in the order of $L/250$ (see Fig. 2).

2) In the design of diagonals and battens, the stiffness requirement must be satisfied in addition to the strength requirement.

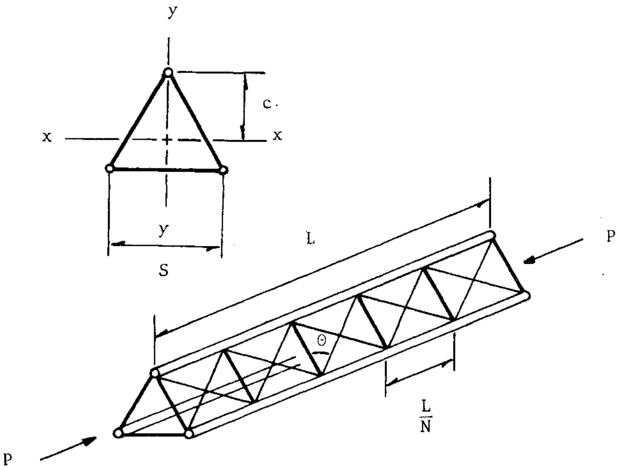

Fig. 1 Geometry of a tubular laced column.

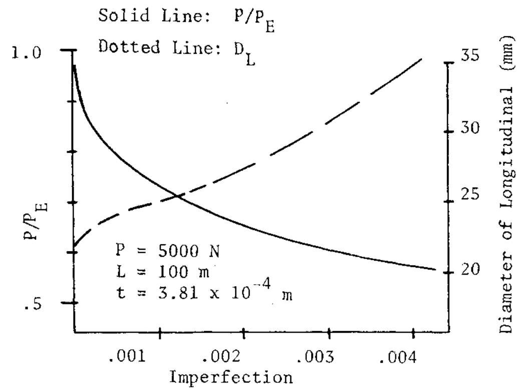

Fig. 2 Reduction of buckling load vs imperfection.

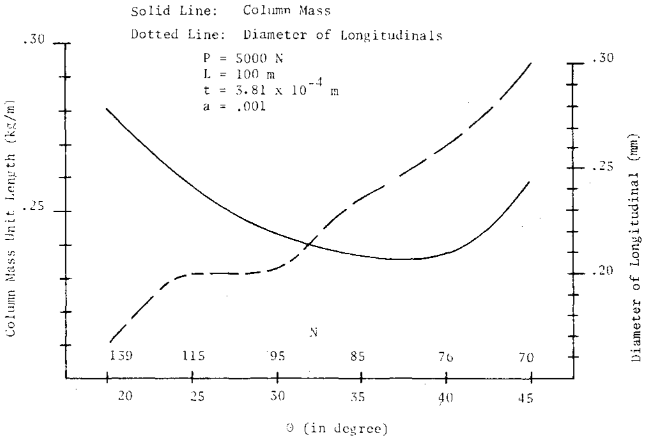

Fig. 3 Variation of column mass vs diagonal angle.

3) The number of bays increases following the column length; however, most of the angles between diagonals and battens are clustered within 35-40 deg regardless of the number of bays.

4) The use of an angle larger than 40 deg is followed with rapid mass penalties for the overall column, whereas penalties are somewhat slower in the ranges of smaller angles than 35 deg (see Fig. 3).

5) More study is needed in developing a rational method for the design of diagonals in regard to shear deformation effect.

6) The column mass resulting from the proposed configuration is lightest among several lightly loaded column concepts comparatively shown in Fig. 4.

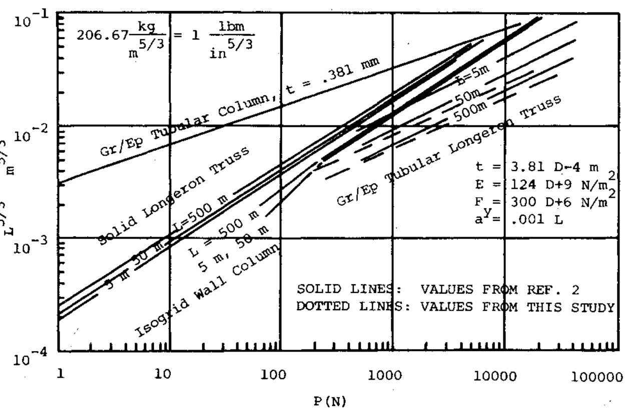

Fig. 4 Masses of several lightly loaded column concepts as a function of design loads.

Acknowledgment

The author would like to express his gratitude to NASA and ASEE for granting the Summer Faculty Fellowship, thereby making this study possible.

References

[1] "NASA SPS Recommended Baseline Systems Concepts," Presentation for July 13, 1978; DOE/NASA SPS Concept Development and Evaluation Program, Preliminary Draft, June 28, 1978.

[2] Mikulas Jr., M.M., "Structural Efficiency of Long Lightly Loaded Truss and Isogrid Columns for Space Applications," NASA Tech. Memo. 78684, Langley Research Center, Hampton, Va., July 1978.

[3] Timoshenko, S.P. and Gere, J.M., *Theory of Elastic Stability*, 2nd Ed., McGraw-Hill Book Co., Inc., New York, 1961, pp. 32-36.

[4] "NASA Space Vehicle Design Criteria: Buckling of Thin-Walled Circular Cylinders," NASA SP-8007, Aug. 1968, pp. 5-6.

[5] Bleich, F., *Buckling Strength of Metal Structures*, McGraw-Hill Book Co., Inc., New York, 1952, pp. 169-175.

[6] Salmon, C. and Johnson, J., *Steel Structures, Design and Behavior*, Intext, 1971, pp. 466-470.

[7] Shanley, F.R., *Weight-Strength Analysis of Aircraft Structures*, 2nd ed., Dover, New York, 1960, pp. 15-20.

[8] "Space Construction Automated Fabrication Experiment Definition Study (SCAFEDS)," Final Rept., NASA Contract No. NAS9-15310, General Dynamics, Convair Division, May 1978, pp. 4-29.

Direct Solutions for Sturm-Liouville Systems with Discontinuous Coefficients

Dewey H. Hodges*
U.S. Army Research and Technology Laboratories (AVRADCOM), NASA Ames Research Center, Moffett Field, Calif.

Introduction

IN a recent paper,[1] direct analytical solutions were obtained for vibrating systems with discontinuities using the method of Ritz. The methodology is based on the use of simple power series and the results can be made as accurate as desired. In this paper, the method is applied to a class of problems described by the Sturm-Liouville equations with discontinuous coefficients. Exact solutions for a class of these problems are presented in Ref. 2. The present results are compared with the exact solutions for various values of system parameters, boundary conditions, and number of terms in the power series.

Received Aug. 7, 1978; revision received March 16, 1979. This paper is declared a work of the U.S. Government and therefore is in the public domain.

Index categories: Structural Dynamics; Heat Conduction; Vibration.

*Research Scientist, Rotorcraft Dynamics Division, Aeromechanics Laboratory. Associate Fellow AIAA.

Statement of the Problem

The problem treated is an eigenvalue problem of the Sturm-Liouville type. Longitudinal vibrations of a nonuniform beam are analyzed to illustrate the method. Similar eigenvalue problems arise from torsional vibrations of nonuniform beams and heat conduction through layered composite materials. Hamilton's law of varying action[1] yields the following expression when simple harmonic motion is assumed:

$$\int_0^L \left(EA\frac{d\bar{u}}{d\bar{x}}\frac{d\delta\bar{u}}{d\bar{x}} - \omega^2 m\bar{u}\delta\bar{u}\right)d\bar{x} = 0 \tag{1}$$

where EA is the longitudinal stiffness, m is the mass per unit length, ω is the frequency of oscillation, and $\bar{u}$ is the longitudinal deflection. An appropriate scaling is:

$$u = \frac{\bar{u}}{L};\ x = \frac{\bar{x}}{L};\ \lambda^2 = \frac{m_r L^2 \omega^2}{EA_r};\ \kappa = \frac{EA}{EA_r};\ c = \frac{m}{m_r} \tag{2}$$

where EA_r and m_r are arbitrary reference values of EA and m.

Equation (1) with $u' = du/dx$, now becomes

$$\int_0^1 (\kappa u'\delta u' - \lambda^2 c u \delta u)\,dx = 0 \tag{3}$$

Since Eq. (3) can be written as a minimum principle, we know that the eigenvalues will be upper bounds when the method of Ritz is applied. The Euler equations and boundary conditions, although not required for the direct solution, may be found by integrating Eq. (3) by parts

$$-\int_0^1 [(\kappa u')' + \lambda^2 c u]\delta u\,dx + \kappa u'\delta u\big|_0^1 = 0 \tag{4}$$

Note that geometric boundary conditions only affect the dimensionless displacement u whereas natural boundary conditions affect the dimensionless tension force $\kappa u'$. In the direct solution, only geometric conditions need to be satisfied by the admissible functions. The following cases are considered:

$$\begin{aligned} &u(0) = u(1) = 0 && \text{case 1} \\ &u(0),\ u(1)\ \text{free} && \text{case 2} \\ &u(0) = 0,\ u(1)\ \text{free} && \text{case 3} \end{aligned} \tag{5}$$

Because of Eq. (4), case 2 implies that $\kappa(0)u'(0) = \kappa(1)u'(1) = 0$, and case 3 implies that $\kappa(1)u'(1) = 0$. It is important to emphasize, however, that Eqs. (5) are the only boundary conditions that need to be satisfied by the admissible functions.

The problem to be considered also has discontinuous coefficients κ and c. Let us assume that the coefficients κ and c are constant within each of M segments, where segments are designated to begin and end at discontinuities in either κ and c. Thus, we designate

$$\kappa = \kappa_k \qquad c = c_k \tag{6}$$

in the kth segment, which has length ℓ_k.